Electronic Supplementary Material (ESI) for RSC Advances.

Supporting Information

A new boat-like tungstoarsenate functionalized by carboxyethyltin and its catalytic properties

Li-Ping Ji,[a] Jing Du,[a] Jian-Sheng Li,[a] Lan-Cui Zhang,*[,a] Xiao-Jing Sang,*[,a,b] He Yang[a], Hong-Juan Cui,[a] Zai-Ming Zhu*[,a]

1. Experimental section

Materials and instrumentation

All reagents and chemicals were purchased from commercial sources and used without further purification. $K_{14}[As_2W_{19}O_{67}(H_2O)]\cdot nH_2O$ [S1] ($\{As_2W_{19}\}$) and the organotinprecursor$Cl_3SnCH_2CH_2COOCH_3$ [S2]were synthesized accordingto the published procedures. All of them were characterized by IR spectroscopy. C, H and N elemental analyses were performed on aVario Elcube elemental analyzer, and Na, K, As, Snand W wereanalyzed on a Prodigy XP emission spectrometer. The IRspectra was recorded using KBr pellets on a Bruker AXSTENSOR-27 FTIR spectrometer in the range of 4000-400 cm^{-1}. TG analysis was performed on a Pyris Diamond TG-DTAthermal analyzer at a heating rate of 10 °C min^{-1}in an airatmosphere. Single crystal X-ray diffraction data was collectedon a Bruker Smart APEX II X-diffractometer equipped withgraphite-monochromated Mo Kα radiation (λ = 0.71073 Å). X-ray powder diffraction (XRPD) data was collected on a BrukerAXS D8 Advance diffractometer using Cu Kα radiation (λ =1.5418 Å) in the 2θ range of 5-50° with a step size of 0.02°. UV-visible spectra was recorded on a Lambda 35 UV-vis spectrophotometer. A CHI 604B electrochemical workstation was used to control the electrochemical measurementsand collect data. A conventional three electrode system wasused. The working electrode was a glassy carbon electrode. Ag/AgCl was used as a reference electrode, and platinum wire wasused as a counter electrode.The yield of cyclohexanone was confirmed on a JK-GC112A Gas Chromatograph. The CEL-HXF300 300W Xe lamp (λ = 420-780 nm) was used to irradiate the light source of photocatalysis.

Synthesis of 1

$Cl_3SnCH_2CH_2COOCH_3$ (0.1 g, 0.32 mmol) and $\{As_2W_{19}\}$ (0.5 g) were dissolved in 30 mL of a pH 6.0 NaAc-HAc buffer solution with vigorous stirring,and the mixture was stirred for 5 h at 90 °C. After cooling to ambient temperature, the insoluble material was filtered off and the clear filtrate was treated with 2.0 g KCl,and 1.5 mL of a 1 mol L^{-1} aqueous $C(NH_2)_3Cl$ solution. Slow evaporation at 50 °C led to the appearance of colorless crystalline compound**1** after about 20 days (Yield: ca.54% based on W). Elemental analysis, Found: C2.13, H 1.01, N0.57, Na 3.16, K 3.74, As 2.05, Sn 6.54, W 55.52. Calc. for $C_{13}H_{73}As_2K_7Na_{10}N_3O_{115}Sn_4W_{22}$: C 2.14, H 1.00, N0.58,Na 3.16, K 3.76, As 2.06, Sn 6.52, W 55.53. IR (KBr, cm^{-1}):3444(s), 3143(s), 2923(w), 2862(w), 1628(s), 1400(s), 1118(w), 945(s), 883(s), 787 (s), 694(s), 474(w).

Oxidation of cyclohexanol to cyclohexanone

The typical procedure for the oxidation catalytic synthesis is: the catalyst (**1**) was added to a mixture of cyclohexanol and acetonitrile in a 100 mL three-necked round-bottom flask equipped with a reflux condenser, and 30% H_2O_2 was dropwise added to the mixture under refluxing conditions (*ca*. 80 °C) over 3.5 h. After completing the reaction, the solvent acetonitrile was removed by distillation, and thus the organic and inorganic phases could be separated by separatory funnel extraction method, and the catalyst was remained in the reaction vessel. Additionally, the reusability of compound **1** was studied through four runs under optimum reaction conditions. The products obtained were characterized by gas chromatography.

Photocatalytic experiments

The photocatalytic reaction was carried out in a 250 mL reactor attached to an inner radiation type with a 300 Whigh-pressure Xe lamp, using the light filter of 420-780 nm as light source. Circulating water was kept flowing through a jacket between the Xe lamp and the reaction chamber, and the system was open to the air. The photocatalytic activities of the samples wereevaluated by measuring the degradation efficiency of RhB solution after a regular interval Xe light irradiation.Preparation of the catalyst was as follows: 0.006 mmol compound was dissolved in 30.0 mL water and the pH value was adjusted to 3.0, followed by adding a certain amount of tetrabutylammonium bromide (TBA) to balance charges in POMs. In the process of photocatalysis, firstly 5.0 mL the solution suspended in 0.02 mmol L^{-1} RhB aqueous solution (50.0 mL) (RhB to catalyst molar ratio 1:1). Take half the volume of the solution after once degradation (RhB to catalyst molar ratio 1:1).The solution was diluted to the initial volume, while adding RhB to maintain the same concentration. In accordance with this method, the solution was diluted to RhB to catalyst molar ratio 1:16.In the process, when the dye is completely degraded, the dye wasre-added to the system, and the catalyst was used for recycling.The solution was magnetically stirred to ensure the equilibrium in the dark for 30 min. Then, every 30 min, 2.0 mL sample was takenoutfor analysis by UV-vis spectroscopy.

2. Crystal structure

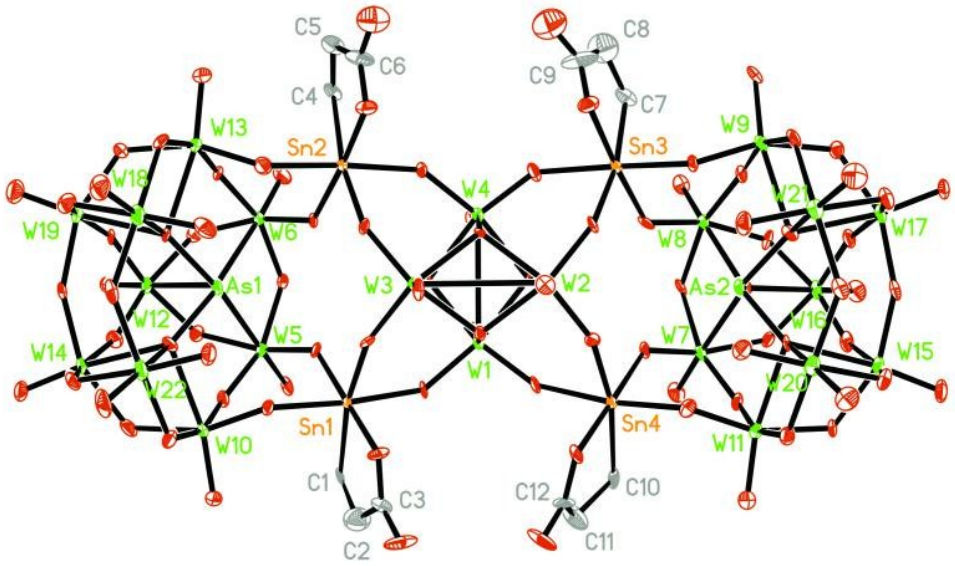

Fig. S1ORTEP drawing of the polyoxoanion of **1**with thermal ellipsoids at 30 % probability (H,K, Na atoms, $[C(NH_2)_3]^+$and free water molecules have been omitted for clarity)

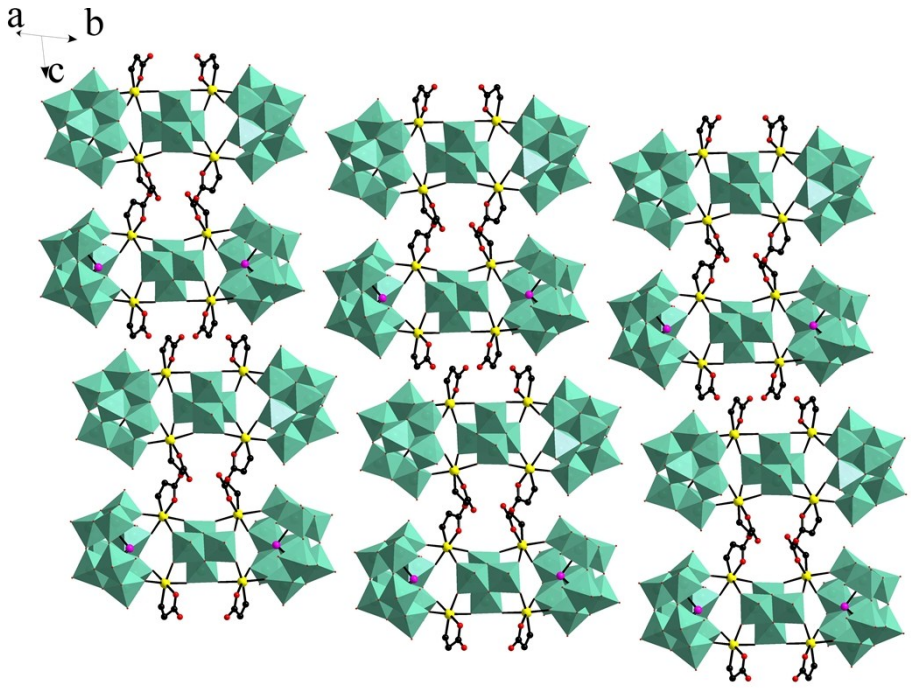

Fig. S2 Polyhedral and ball-and-stick view of the 3D supramolecular framework of **1**(All H atoms, the isolated $[C(NH_2)_3]^+$, K^+, Na^+ and water molecules existing in the interspaces are omitted for clarity)

Table S1. Crystal and refinement data for **1**

Compound	**1**
Formula	$C_{13}H_{72}As_2K_7Na_{10}N_3O_{115}Sn_4W_{22}$
Formula weight	7283.64
T /K	296(2)
Wavelength / Å	0.71073
Crystal system	Monoclinic
Space group	$P\bar{1}$
a, b, c /Å	11.9822(16), 22.500(3), 25.497(3)
α, β, γ /°	69.912(2), 82.904(2), 86.609(2)
V /Å^3, Z	6405.2(15),2
D_c /g cm^{-3}, F_{000}	3.777, 6456
GOF	1.002
Reflections collected	32489
R_{int}	0.0554
θ Range(°)	1.05 to 25.00
$R_1(I > 2\sigma(I))$ [a]	0.0561
wR_2 (all data)[a]	0.1566

[a] $R_1 = \sum||F_0| - |F_C||/\sum|F_0|$; $wR_2 = \sum[w(F_0^2 - F_C^2)^2]/\sum[w(F_0^2)^2]^{1/2}$

Table S2. Selected bond lengths (Å) and angles (º) for **1**

Bond	Length (Å)	Bond	Length (Å)	Bond	Length (Å)
W1–O55	1.734(12)	W11–O49	1.739(14)	W21–O56	1.735(15)
W1–O62	1.780(14)	W11–O2	1.824(15)	W21–O77	1.754(16)
W1–O12	1.832(12)	W11–O1	1.892(13)	W21–O4	1.923(15)
W1–O53	2.057(13)	W11–O15	1.895(13)	W21–O13	1.972(14)
W1–O43	2.071(13)	W11–O58	1.974(14)	W21–O25	2.071(15)
W1–O26	2.228(12)	W11–O31	2.311(12)	W21–O35	2.307(11)
W2–O17	1.747(12)	W12–O39	1.723(14)	W22–O44	1.689(16)
W2–O76	1.800(13)	W12–O51	1.872(14)	W22–O73	1.747(15)
W2–O33	1.802(12)	W12–O27	1.882(14)	W22–O30	1.944(16)
W2–O65	2.024(12)	W12–O23	1.891(14)	W22–O79	1.976(14)
W2–O26	2.056(12)	W12–O8	1.892(15)	W22–O70	2.086(14)
W2–O43	2.211(12)	W12–O38	2.430(12)	W22–O47	2.301(13)
W3–O42	1.760(12)	W13–O81	1.725(14)	Sn1–O50	2.023(12)
W3–O50	1.809(13)	W13–O29	1.810(15)	Sn1–O72	2.035(13)
W3–O66	1.825(12)	W13–O37	1.873(14)	Sn1–O12	2.049(13)
W3–O26	2.039(13)	W13–O40	1.939(13)	Sn1–O54	2.122(14)
W3–O65	2.054(12)	W13–O11	1.988(15)	Sn1–O83	2.159(13)
W3–O53	2.185(12)	W13–O45	2.321(12)	Sn2–O66	2.036(12)
W4–O67	1.735(14)	W14–O74	1.703(15)	Sn2–O60	2.047(11)
W4–O36	1.782(13)	W14–O70	1.834(13)	Sn2–O71	2.061(14)
W4–O71	1.830(14)	W14–O18	1.920(13)	Sn2–O29	2.131(17)
W4–O43	2.055(12)	W14–O24	1.923(16)	Sn2–O85	2.198(14)

W4–O53	2.080(13)	W14–O27	1.949(14)	Sn3–O33	2.051(13)
W4–O65	2.252(12)	W14–O47	2.411(14)	Sn3–O34	2.059(14)
W5–O68	1.698(13)	W15–O78	1.729(16)	Sn3–O20	2.072(13)
W5–O72	1.821(13)	W15–O19	1.825(13)	Sn3–O36	2.110(14)
W5–O41	1.881(13)	W15–O58	1.902(13)	Sn3–O87	2.207(15)
W5–O52	1.963(13)	W15–O16	1.917(13)	Sn4–O76	2.031(12)
W5–O23	1.972(14)	W15–O63	1.922(14)	Sn4–O7	2.037(13)
W5–O38	2.392(12)	W15–O31	2.433(13)	Sn4–O2	2.090(15)
W6–O80	1.735(14)	W16–O75	1.714(16)	Sn4–O62	2.109(14)
W6–O60	1.846(12)	W16–O28	1.882(13)	Sn4–O89	2.172(13)
W6–O40	1.892(13)	W16–O3	1.888(13)	Sn1–C1	2.098(17)
W6–O52	1.913(13)	W16–O5	1.891(13)	Sn2–C4	2.125(19)
W6–O8	1.979(16)	W16–O63	1.895(15)	Sn3–C7	2.14(2)
W6–O38	2.307(12)	W16–O46	2.407(14)	Sn4–C10	2.15(2)
W7–O32	1.714(13)	W17–O6	1.728(15)	As1–O38	1.770(12)
W7–O7	1.844(13)	W17–O25	1.848(14)	As1–O47	1.796(13)
W7–O57	1.921(13)	W17–O48	1.907(13)	As1–O45	1.803(12)
W7–O15	1.928(13)	W17–O16	1.910(14)	As2–O46	1.786(12)
W7–O28	2.013(15)	W17–O3	1.928(13)	As2–O31	1.783(13)
W7–O46	2.355(12)	W17–O35	2.381(14)	As2–O35	1.808(12)
W8–O59	1.717(13)	W18–O82	1.677(18)	C1–C2	1.513(10)
W8–O34	1.850(14)	W18–O22	1.709(15)	C2–C3	1.48(3)
W8–O61	1.855(12)	W18–O30	1.881(15)	C4–C5	1.519(10)
W8–O57	1.934(12)	W18–O37	1.979(14)	C5–C6	1.525(10)
W8–O5	1.960(14)	W18–O9	2.105(16)	C7–C8	1.519(10)
W8–O46	2.331(13)	W18–O45	2.313(12)	C8–C9	1.50(4)
W9–O14	1.702(13)	W19–O10	1.707(17)	C10–C11	1.52(3)
W9–O20	1.817(13)	W19–O9	1.851(14)	C11–C12	1.50(3)
W9–O13	1.873(13)	W19–O11	1.904(13)	C3–O83	1.27(2)
W9–O48	1.952(14)	W19–O18	1.907(13)	C3–O84	1.23(3)
W9–O61	1.983(12)	W19–O51	1.945(14)	C6–O85	1.24(2)
W9–O35	2.347(13)	W19–O45	2.387(13)	C6–O86	1.21(3)
W10–O69	1.730(14)	W20–O64	1.744(15)	C9–O87	1.25(3)
W10–O54	1.783(14)	W20–O21	1.745(17)	C9–O88	1.26(4)
W10–O79	1.887(14)	W20–O4	1.899(14)	C12–O89	1.29(2)
W10–O41	1.958(13)	W20–O1	1.967(13)	C12–O90	1.21(3)
W10–O24	1.963(16)	W20–O19	2.108(15)		
W10–O47	2.309(14)	W20–O31	2.317(12)		
Bond	Angle(°)	Bond	Angle(°)	Bond	Angle(°)
O12–W1–O43	159.1(5)	O69–W10–O47	168.5(6)	O9–W19–O45	74.3(6)
O55–W1–O26	164.8(5)	O79–W10–O47	74.1(5)	O11–W19–O45	73.3(5)
O53–W1–O26	73.6(5)	O24–W10–O47	74.7(5)	O64–W20–O19	164.7(6)
O43–W1–O26	73.9(5)	O2–W11–O58	160.3(6)	O21–W20–O31	163.5(6)
O76–W2–O65	158.6(5)	O49–W11–O31	168.3(6)	O1–W20–O31	72.3(5)
O65–W2–O26	73.8(5)	O1–W11–O31	73.7(5)	O19–W20–O31	72.2(5)

O17–W2–O43	166.9(6)	O58–W11–O31	74.8(5)	O4–W21–O13	155.2(6)
O65–W2–O43	74.3(5)	O51–W12–O23	158.9(5)	O77–W21–O25	164.0(6)
O66–W3–O26	160.4(5)	O39–W12–O38	169.9(6)	O13–W21–O35	72.9(5)
O65–W3–O53	75.1(5)	O23–W12–O38	73.8(5)	O25–W21–O35	71.6(5)
O26–W3–O65	73.5(5)	O8–W12–O38	72.4(5)	O44–W22–O70	162.7(7)
O42–W3–O53	165.6(6)	O29–W13–O11	159.7(6)	O73–W22–O47	163.9(7)
O36–W4–O53	157.9(5)	O81–W13–O45	167.4(6)	O79–W22–O47	72.7(5)
O67–W4–O65	164.9(6)	O37–W13–O45	75.2(5)	O70–W22–O47	71.2(5)
O43–W4–O65	72.8(5)	O11–W13–O45	73.5(5)	O72–Sn1–O12	93.0(5)
O53–W4–O65	73.1(4)	O70–W14–O27	158.1(6)	O72–Sn1–C1	104.0(6)
O72–W5–O23	163.0(5)	O74–W14–O47	170.6(6)	O72–Sn1–O54	87.4(5)
O68–W5–O38	167.6(6)	O70–W14–O47	72.7(5)	C1–Sn1–O54	93.9(7)
O52–W5–O38	71.7(5)	O24–W14–O47	72.9(5)	O66–Sn2–O71	84.4(5)
O23–W5–O38	73.4(5)	O19–W15–O63	158.2(6)	O60–Sn2–O29	87.2(5)
O60–W6–O8	163.0(6)	O78–W15–O31	172.2(6)	C4–Sn2–O85	81.5(6)
O80–W6–O38	168.1(6)	O19–W15–O31	74.2(5)	C4–Sn2–O29	97.1(7)
O52–W6–O38	74.5(5)	O58–W15–O31	73.1(5)	O33–Sn3–O20	87.7(5)
O8–W6–O38	73.9(5)	O28–W16–O3	159.3(6)	O33–Sn3–O36	82.0(5)
O7–W7–O28	162.4(5)	O75–W16–O46	170.0(6)	O20–Sn3–C7	96.8(8)
O32–W7–O46	168.6(6)	O28–W16–O46	74.4(5)	C7–Sn3–O87	82.0(7)
O57–W7–O46	72.7(5)	O5–W16–O46	72.1(5)	O7–Sn4–O2	88.2(5)
O28–W7–O46	73.7(5)	O25–W17–O3	158.6(6)	O76–Sn4–O62	83.1(5)
O34–W8–O5	162.6(6)	O6–W17–O35	170.3(6)	O2–Sn4–C10	97.2(7)
O59–W8–O46	165.0(6)	O25–W17–O35	73.6(5)	C10–Sn4–O89	80.3(7)
O57–W8–O46	73.0(5)	O48–W17–O35	73.0(5)	O38–As1–O47	98.5(6)
O5–W8–O46	72.8(5)	O82–W18–O9	164.9(6)	O38–As1–O45	96.9(6)
O20–W9–O48	158.9(6)	O22–W18–O45	164.2(7)	O47–As1–O45	95.2(6)
O14–W9–O35	167.6(6)	O37–W18–O45	73.6(5)	O31–As2–O461	97.4(6)
O13–W9–O35	73.6(5)	O9–W18–O45	71.7(5)	O46–As2–O35	96.9(6)
O48–W9–O35	73.1(5)	O9–W19–O51	159.2(6)	O31–As2–O35	96.0(6)
O54–W10–O24	159.7(6)	O10–W19–O45	171.8(6)		

3. Physical characterizations

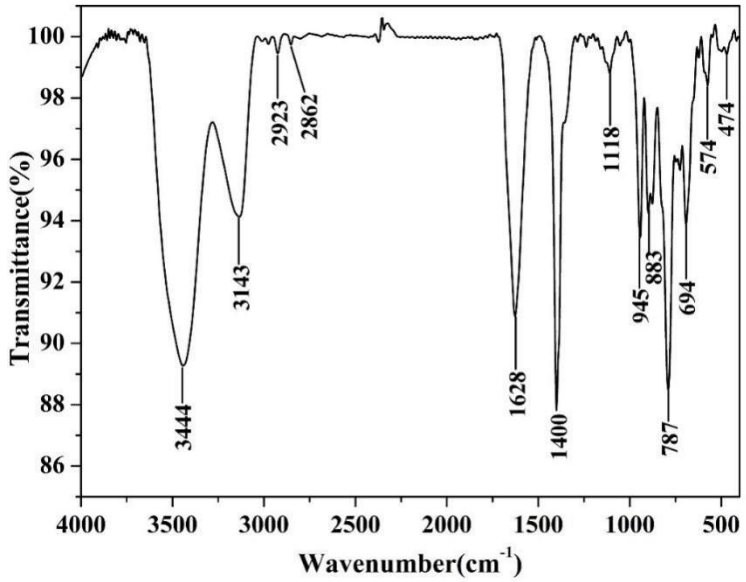

Fig. S3 The IR spectrum of **1**

IR spectrum of **1** further confirmed the successful introduction of carboxyethyltin group. As shown in Fig. S3, the peaks at 2923, 2862 cm^{-1} for **1** can be attributed to the characteristic vibrations of the organic group ($–CH_2$), while the sharp peaks at 1400 and 1628 cm^{-1} for **1** are attributed to the stretching vibration of –COO.[S3] The appearance of the peaks at 474 and 574 cm^{-1} for **1**can be regarded as symmetric vibration of Sn–C bond. Moreover, the peaks between 1030 and 760 $cm^{-1}$are assigned to the characteristic vibrations of POMs, the peaksat 945, 883, 787, 694 $cm^{-1}$for **1** areattributed to the asymmetric stretching vibrations of W–O_t and W–O_b,c (O_t and O_b /O_c represent terminal and bridging O atoms).The As–O stretching peak is located at about1118 cm^{-1}.

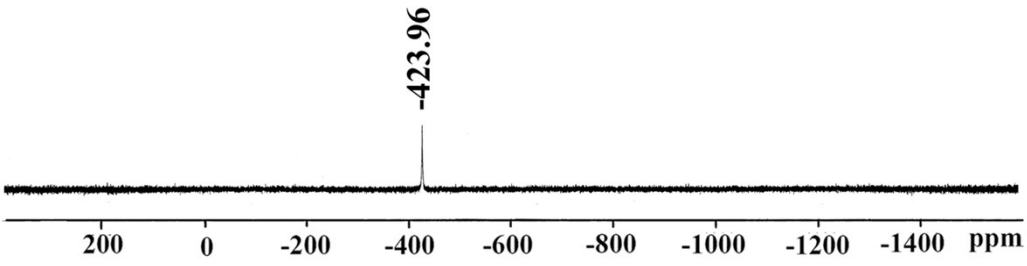

Fig. S4 The ^{119}Sn NMR of $Cl_3Sn(CH_2)_2COOCH_3$ in $D_2O/(CH_3)_4Sn$

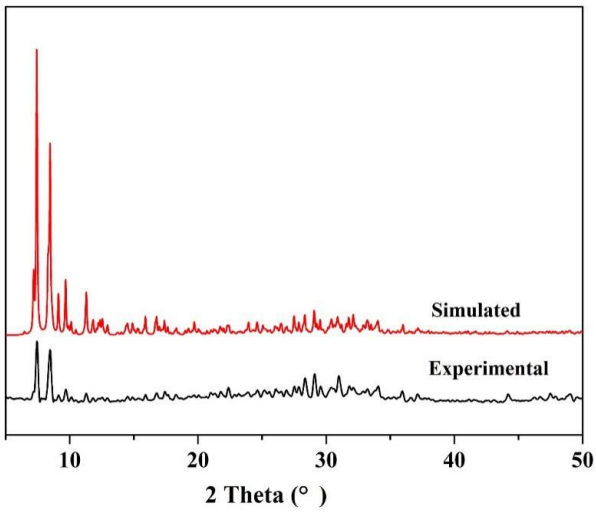

Fig. S5 The simulated and experimental XRD patterns of **1**

The purity of the as-synthesized compound was evaluated by XRPD patterns for experimental and simulated results of **1** in Fig. S5, which illustrated the diffraction peaks of two patterns match well, indicating its good phase purity. The difference ofintensity is probably due to the variation in preferred orientation of the powder sample during collection of the experimental XRPD pattern.

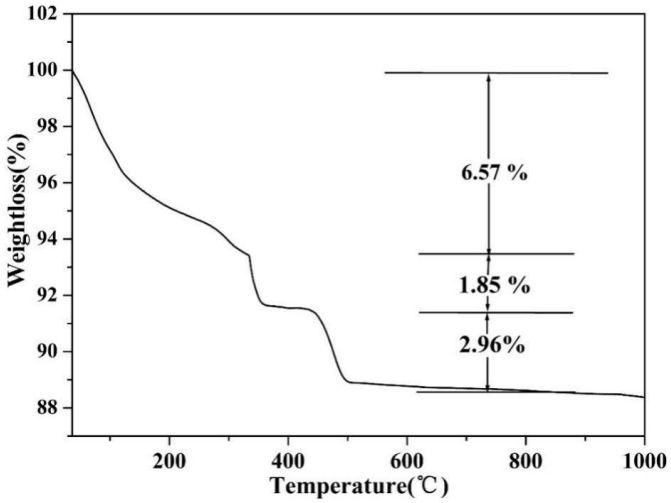

Fig. S6 TG curve of **1**

This carboxyethyltin-POM hybrid shows good thermal stability. From the TG analysis (Fig. S6) we can see that the introduced $(CH_2)_2COO^-$ group can be stable until 333 °C, in which there are three continuous weight loss steps from 35 to 800 °C for the title compound. The first weight loss of 6.57% (calcd. 6.20%) occurring from 35 to 333 °C corresponds to the loss of all lattice water molecules. The second weight loss of 1.85% (calcd. 1.82%) in the temperature range of 333-442 °C is attributed to the removal of one $[C(NH_2)_3]^+$ organic cation and one $(CH_2)_2COO^-$ group. Further, the compound continuously lost weight of 2.96% (calcd. 2.97%) at higher temperatures of 442-800 °C, which is mainly attributed to the loss of three $(CH_2)_2COO^-$ groups. Within the temperature range of 800-1000 °C, the weight remains almost the same, inferring the polyoxoanion skeleton of **1** is stable.

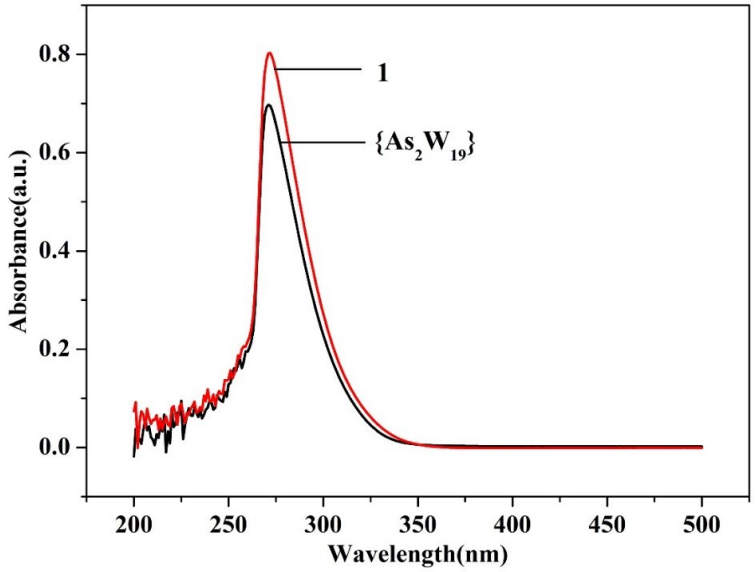

Fig. S7 The UV-vis absorption spectrum of **1**and its parent $\{As_2W_{19}\}$

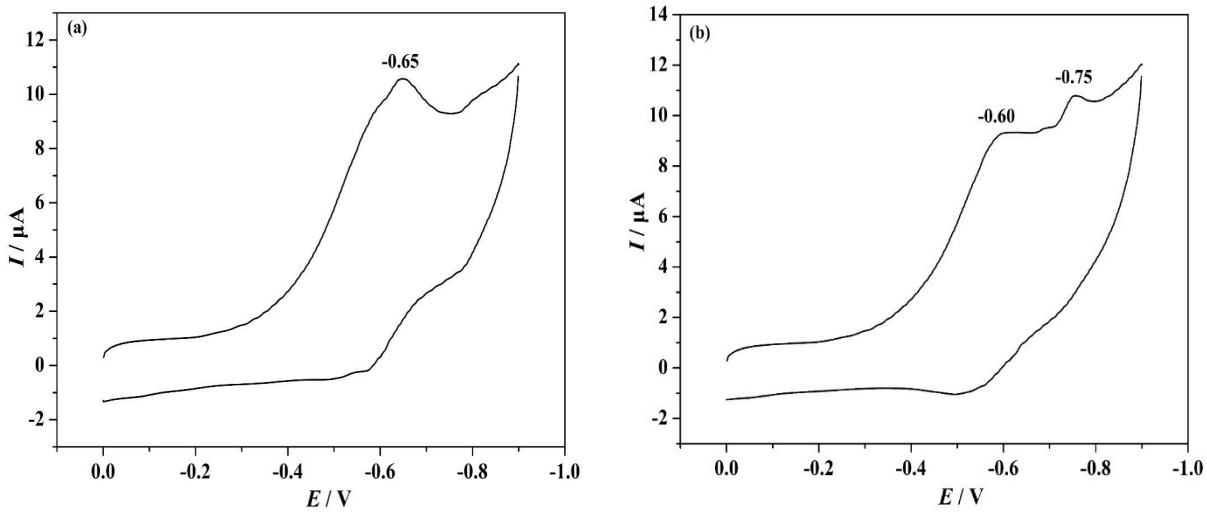

Fig. S8 Cyclic voltammetry curves of $\{As_2W_{19}\}$ (a) and **1** (b) in pH 3.0 Na_2SO_4-H_2SO_4 buffer solution

The redox property of **1**was evaluated by cyclic voltammetry in Na_2SO_4-H_2SO_4 solution with pH = 3. As shown in Fig. S8, two cathode peaks were observed in the range from 0 to -1.0 V for **1**, indicating stepwise reduction processes, whereas only one cathode peak appeared for $\{As_2W_{19}\}$. Furthermore, their redox processes are irreversible.

4. Catalytic tests

(1) The catalytic oxidation of cyclohexanol to cyclohexanone

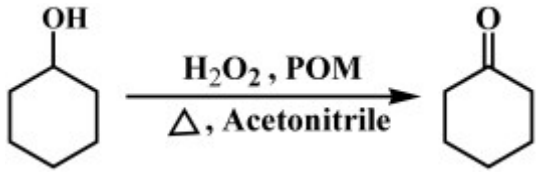

Scheme S1 Theoxidationprocess of cyclohexanone to cyclohexanol catalyzed by POMs

(2) The mimic enzyme catalysis

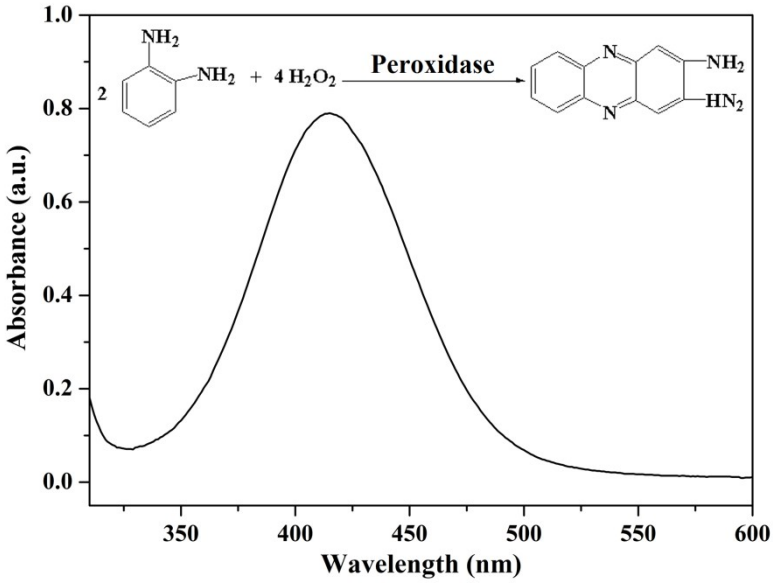

Fig.S9 The UV-vis absorption spectrum of the resulted reaction solution of OPD catalyzed by **1**

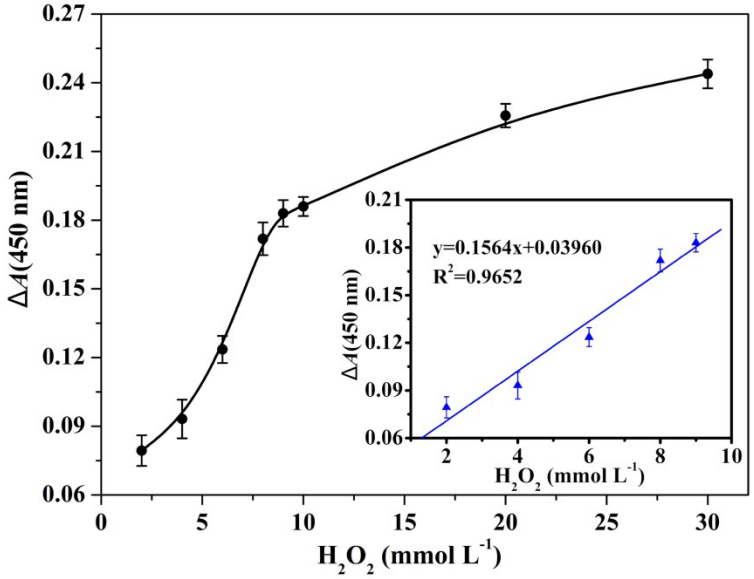

Fig. S10 The linear calibration plot for H_2O_2detection, Δ*A*= *A* (**1**, 450nm)–*A*(blank, 450nm),the error bars represent thestandard deviation of three measurements

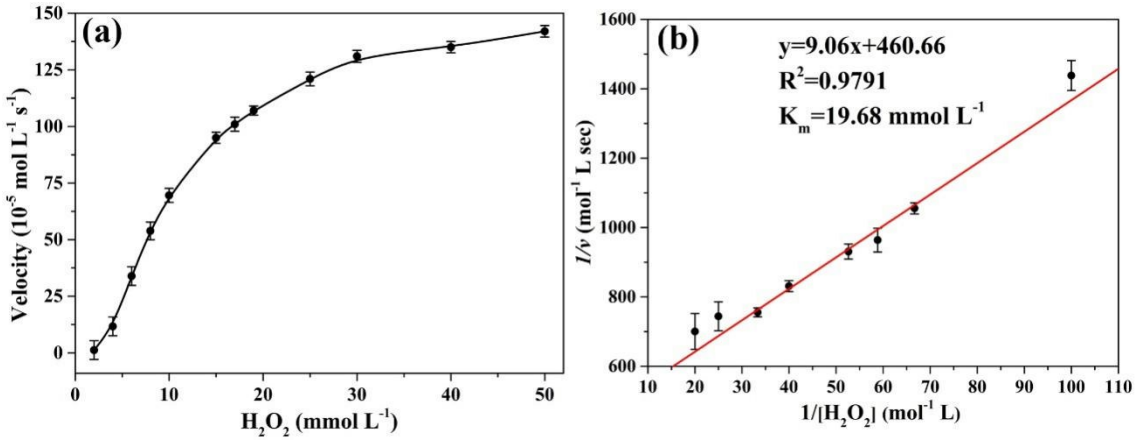

Fig. S11 The kinetic analysis (a) and Lineweaver-Burk plots (b) of compound **1** with H_2O_2 as substrate

The steady state kinetics was performed by varying the concentration of H_2O_2 (2-50 mmol L^{-1}) at fixed concentration of compound **1** (3 mg) and OPD (2.5 mmol L^{-1}). The reaction was conducted in 1 mL acetate buffer (pH = 4.0) and the variation of absorbance was monitored as function of time in 2 min at 450 nm ($\varepsilon = 1.26 \times 10^5$ mol L^{-1} cm^{-1}). The apparent kinetic parameters were calculated based on the Lineweaver-Burk equation, $1/V = K_m/V_{max} \times [S] + 1/V_{max}$, V is the velocity, V_{max} is the maximum velocity, K_m is the Menten constant, [S] is the concentration of H_2O_2.[S4]

(3) The visible photocatalytic degradation of organic dye RhB

Table.S3 Effect of catalyst dosage of compound **1** on photocatalytic degradation efficiency with 50 mL 0.02 mmol L^{-1} RhB solution

Entry	*n*(catalyst/RhB)	Time(h)	Degradation rate (%)	Degradation rate (%)	
				Recycle I	Recycle II
1	1:1	1.5	95	99	98
2	1:2	2	97	98	98
3	1:4	3	98	97	96
4	1:8	4	94	97	97
5	1:16	6	95	95	96

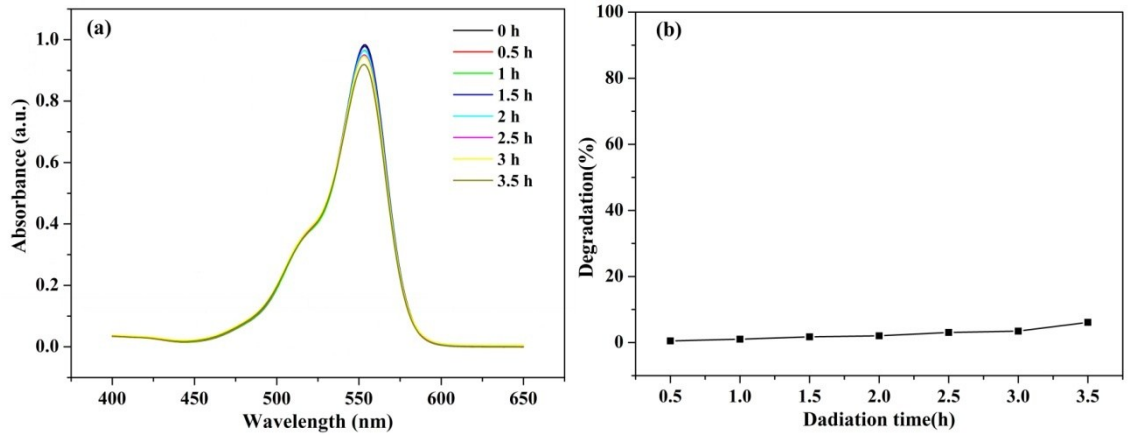

Fig. S12 Photocatalytic degradation of RhB without **1** (a) and plot of degradation of RhB versus irradiation time undervisible light without**1** (b)

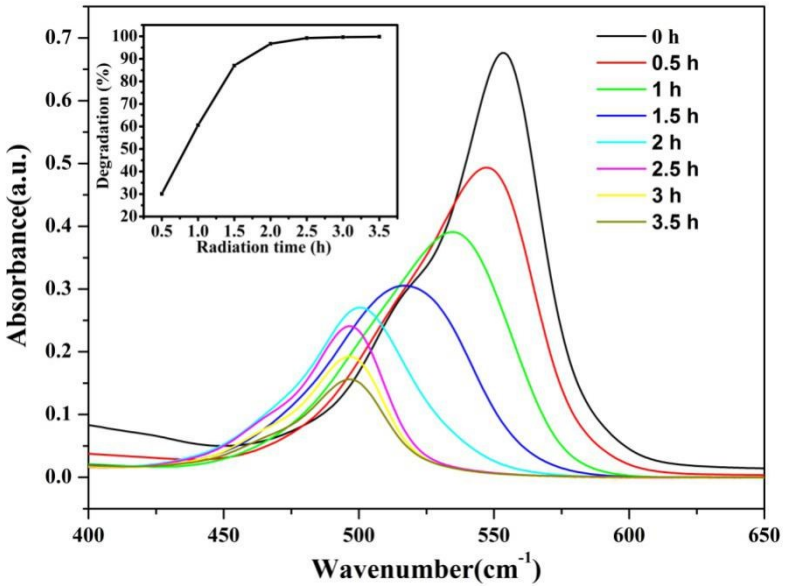

Fig. S13 UV-vis absorption spectra of RhB solution during the decomposition process under visible light in the presence ofthe parent $\{As_2W_{19}\}$. The inset is thecorresponding degradation versus reaction time

References

[S1] U.Kortz, M. G. Savelieff, B. S. Bassil and M. K. Dickman, *Angew. Chem. Int. Ed.* 2001, **40**, 3384-3386.

[S2] R. E.Hutton, J. W. Burley and V. Oakes, *Organomet. Chem.* 1978, **156**, 369-382.

[S3] (*a*) M. K. Rauf, M. A. Saeed, Imtiaz-ud-Din. M. Bolte, A. Badshah, B. J. Mirza, *Organomet. Chem*. 2008, **693**, 3043-3048; (*b*) J. W. Zhao, J. Zhang, Y. Song, S. T. Zheng and G. Y. Yang, *Eur. J. Inorg. Chem.* 2008, **2008**, 3809-3819.

[S4]J. A. Nicell and H. Wright, Enzyme Microb. Tech., 1997, **21**, 302-310.